Evaluation and Optimisation of Three-Point Hitch Geometry of MF475 Tractor

N. Moradinejad[1*]

1- Department of Mechanics of Biosystems Engineering, Ta. C., Islamic Azad University, Tabriz, Iran
(*- Corresponding Author Email: n.morad@iau.ac.ir)
https://doi.org/10.22067/jam.2025.95018.1422

Abstract

In recent years, the adoption of agricultural tractors has advanced farm mechanisation, with the three-point hitch (TPH) system playing an important role in attaching implements. This study focuses on optimising the geometry of the TPH for the Massey Ferguson 475 (MF475) tractor through simulation in SolidWorks software and validation with laboratory measurements. The independent parameters, including (1) lift arm, (2) lift rod, (3) lower arm lengths, and (4) the distance between the lift rod-lower arm connection point and the lower arm pivot point, were systematically varied to find the optimal design. Additionally, we analysed the effects of the independent parameters on performance parameters such as virtual hitch point positions, mechanical advantage, and lifting force. Results indicated that the existing TPH of the MF475 tractor exhibits discrepancies from the ASABE standard, while the optimised design complies with it. The results showed that the length of the lower arms has the greatest influence on the position of the virtual hitch point. Additionally, the increase in the lengths of the lift arm, lift rod, and lower arm led to a decrease in the lifting forces. In contrast, the increase in the distance between the lift rod-lower arm connection point and the lower arm pivot point led to an increase in the lifting forces. Sensitivity analysis revealed that the distance between the lift rod-lower arm connection point and the lower arm pivot point is the most influential factor affecting lifting force and mechanical advantage.

Keywords: Lifting force, Mechanical advantage, Simulation, Solid-Works, Virtual hitch point

Nomenclature

L_1	Lift arm length	$MF475$	Massey Ferguson tractor model 475
L_2	Lift rod length	l_b , l_u	Lower and upper ranges of the distance between the end of PTO and the lower arm endpoint (when the lower arm is horizontal)
L_3	Distance between the lift rod-lower arm connection point and the lower arm pivot point	l_{14}	Lower arm endpoint height
L_4	Lower arm length	l_{15}	Levelling alignment
L_5	Upper arm length	l_{18}	Movement range
P1	Pivot point of the lift arm	l_{19}	Transport height
P2	Lift arm and lift rod connection point	l_{20}	Lower arm endpoint clearance
P3	Lift rod and lower arm connection point	r_{wr}	Rear wheel radius
P4	Lower arm pivot point	F_{P1x}, F_{P1y}	Horizontal and vertical components of the force on the lift arm
P5	Lower arm endpoint	F_{P4x}, F_{P4y}	Horizontal and vertical components of the force on the lower arms
P6	Upper arm pivot point	F_{LR}	Lift rod force
P7	Upper arm endpoint	F_{lift}	Force at the lower arm endpoint
θ	Lift arm angle with respect to the horizon	M_{P1}	Moment about point P_1
α	Lower arm angle with respect to the horizon	TPH	Three-point hitch
β	Upper arm angle with respect to the horizon	VHP	Virtual hitch point
φ_1	Angle between the lift arm and the lift rod	MA	Mechanical advantage
φ_2	Angle between the lift rod and the lower arm	(X_{VHP}, Y_{VHP})	Coordinates of the virtual hitch point with respect to the rear axle centre
MH	Mast height	L_{CV}	Vertical convergence distance

Introduction

Over the past decade, the widespread adoption of agricultural tractors has played a pivotal role in advancing farm mechanisation, thereby significantly enhancing agricultural productivity (Dhruw, Pareek, & Singh, 2018; Pranav, Kumar, Ansh, & Kumar, 2024). From the earliest tractor models, establishing a reliable and effective connection between tractors and implements has been a critical challenge. Initially, towing hitches were employed; however, these posed risks related to instability, diminished traction efficiency, and compromised safety. A landmark advancement came with Ferguson's introduction of the three-point hitch (TPH) system in 1935, which has since become the universal standard for attaching implements to tractors (Molari, Mattetti, & Guarnieri, 2014). The TPH consists of two lower and one upper articulated links, combined with a hydraulically operated load and position control system, as incorporated in Ferguson's original patent (Pásztor & Popa-Müller, 2021). This system enhances the tractive efficiency of two-wheel drive tractors by dynamically transmitting weight to the rear wheels when an implement is pulled (Avello Fernández, Maraldi, Mattetti, & Varani, 2022; Molari *et al.*, 2014). Over time, the TPH has evolved to include features such as position control for improved transport comfort and quick-hitch mechanisms to facilitate easier implement attachment (Chukewad *et al.*, 2024; Jeon *et al.*, 2019).

Considerable research efforts have focused on optimising the geometry of the TPH to conform to the standard specifications defined by ISO 730 (ISO, 2009) and ASABE Standard S217.12 (ASABE Standards, 2007). One principal objective of this optimisation is to improve the lifting capacity, a critical performance metric utilised by manufacturers to define TPH capability (Molari *et al.*, 2014). The lifting force is measured according to OECD Code 2 standards (OECD, 2012), which specify testing both with and without an attached frame to determine the maximum lifting force.

In pursuit of optimal TPH geometry, Ambike and Schmiedeler (2007) applied Geometric Constraint Programming to identify kinematic configurations that satisfy ASABE S217.12 constraints, complemented by a CAD-based visualisation tool to illustrate the effects of design parameters. Similarly, Pranav *et al.* (2024) developed a computational program able to position the virtual hitch point according to the operating depth, optimising the geometry with the goal of positioning the hitch point along the line of pull. Prasanna Kumar (2012) utilised the Newton-Raphson method to analyse the linkage range of motion and the paths of hitch points. This study was further advanced by generating hitch point trajectories and calculating geometric performance parameters, as well as mechanical advantage, using data from 165 TPHs reported in Nebraska tractor tests. Dhruw *et al.* (2018) evaluated the performance of the TPH system by developing a Visual Basic program. Their study traced the locations of the upper, lower, and virtual hitch points during the lift arm's power travel. They concluded that the length of the lift rod most strongly affected the mechanical advantage of the hitch system.

Molari *et al.* (2014) proposed a constrained optimisation method that maximises the lifting force according to OECD Code 2, while adhering to ISO 730 standard requirements. The proposed design tool was verified using an existing three-point linkage configuration, and the results demonstrated a substantial increase in maximum lifting force compared to the original design. Sensitivity analysis identified the lift arm length, lower arm length, and the positions of their pivot points as the most influential variables affecting performance.

Bauer, Porteš, Slimařík, Čupera, and Fajman (2017) investigated the influence of TPH setup on rear wheel load distribution during in-furrow ploughing, revealing that adjusting the upper arm length significantly reduced load imbalances. Their study underscored the role of the TPH in load transmission to the tractor but emphasised the TPH setup rather than its structural optimisation for dynamic tractor behaviour.

Advancements in computer-aided design tools have greatly facilitated system analysis and optimisation, eliminating the need for costly and labour-intensive experimental testing. Historically, researchers have developed simulation tools using Visual Basic programming (Dhruw *et al.*, 2018; Singh & Pandey, 2017). Moreover, SolidWorks, a three-dimensional solid modelling design program, is most commonly used worldwide, open to development, easy to use, and able to work comfortably with Windows applications. It provides the user with the flexibility to select and incorporate various design parameters into the test system and analyse their consequences on the system's performance. Employing SolidWorks for system design enables detailed geometric characterisation and standards compliance assessment, thus providing an accessible and cost-effective method for researchers and manufacturers (Padhiary, Roy, & Kumar, 2025; Selech *et al.*, 2019; Selvi & Kabas, 2018; Wu, Zhang, & Wang, 2019).

Despite extensive global research on TPH optimisation, a critical need remains to evaluate and optimise the three-point hitch systems in tractors manufactured by the Iranian Tractor Manufacturing Co. (ITMCo) to ensure compliance with established standards and enhance their operational performance. Accordingly, this study aims to utilise SolidWorks software to optimise the TPH geometry of MF475 tractors, with particular emphasis on adherence to ASABE standards. The simulated TPH designs are validated through laboratory tests to ensure accuracy and reliability.

Materials and Methods

The Massey Ferguson tractor Model 475 (Fig. 2), manufactured by the ITM Company, is more common in Iran compared to other tractors. This model is equipped with a 4-cylinder diesel engine featuring direct injection and a wheelbase of 2290 mm. Its hydraulic system produces an approximate lifting capacity of 2,227 kg (Anonymous, 2020).

The TPH system of the MF475 Tractor consists of one internal hydraulic cylinder that transfers lifting force to the lift arms by rotating the rock shaft. This system is classified as Category I and II. In the x-y plane, the TPH system is a six-bar mechanism modelled as two distinct four-bar linkages. The first four-bar linkage comprises the lift arm (1), the lift rod (2), the lower arm (3), and the tractor body (5). The second four-bar linkage consists of the lower arm (3), the implement frame (6), the top link (4), and the tractor body (5) (Fig. 1; Molari *et al.*, 2014; Dhruw *et al.*, 2018). Precisely adjusting the hitch parameters is essential for maximising the lifting capacity of the TPH system while simultaneously ensuring compliance with ASABE standards.

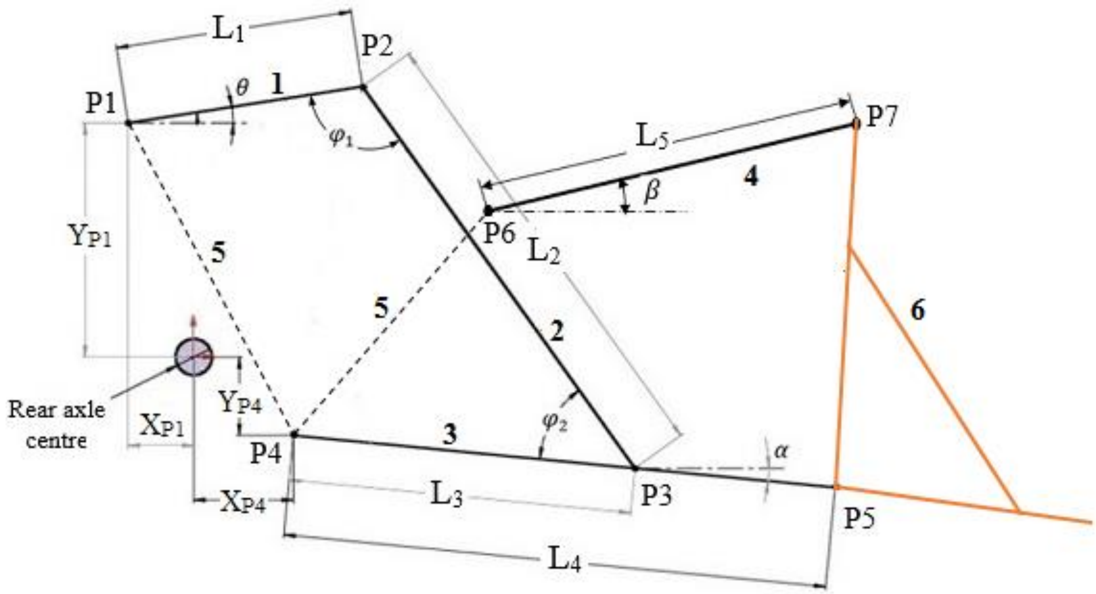

Fig. 1. Components of the TPH system: 1= Lift arm, 2= Lift rod, 3= Lower arm, 4= Upper arm, 5= Tractor body, 6= Implement, L_1= Lift arm length, L_2= Lift rod length, L_3= Distance between the lift rod-lower arm connection point and the lower arm pivot point, L_4= Lower arm length, L_5= Upper arm length, θ= Lift arm angle with respect to the horizon, α= Lower arm angle with respect to the horizon, β= Upper arm angle with respect to the horizon, φ_1=Angle between the lift arm and the lift rod, φ_2= Angle between the lift rod and the lower arm, P1= Pivot point of the lift arm, P2= Lift arm and lift rod connection point, P3= Lift rod and lower arm connection point, P4= Lower arm pivot point, P5= Lower arm endpoint, P6= Upper arm pivot point, P7= Upper arm endpoint.

Laboratory measurements

To measure the heights of the lift arm endpoints as well as the lower and upper arm connection points to the plough in both raising and lowering modes, a chisel plough was attached to the tractor. All measurements were taken on flat-level ground using a tape measure with millimetre accuracy, with the rear axle centre as the reference origin. To minimise measurement errors, the tape measure was affixed to a wooden board and utilised as a set square ruler (Fig. 2).

Fig. 2. Laboratory test setup on the Massey Ferguson tractor Model 475: 1= Chisel plough, 2= Set square ruler, 3= Connection pin between the lower arm and chisel plough.

Solid-Works simulation

SolidWorks has three main sections: the Part Module, the Assembly Module, and the Drawing Module. The part module facilitates modelling and designing individual system components. The assembly module enables the integration of these components and supports motion studies on the assembled system. Three types of motion studies are available: animation, basic motion, and motion analysis.

In this study, we used SolidWorks motion simulation on the TPH system to find the motion range of the lift arm and hitch points, as the system is symmetrical with respect to the tractor's x-y plane. We designed each TPH part in the part module and then assembled all the components into a single file (Fig. 3).

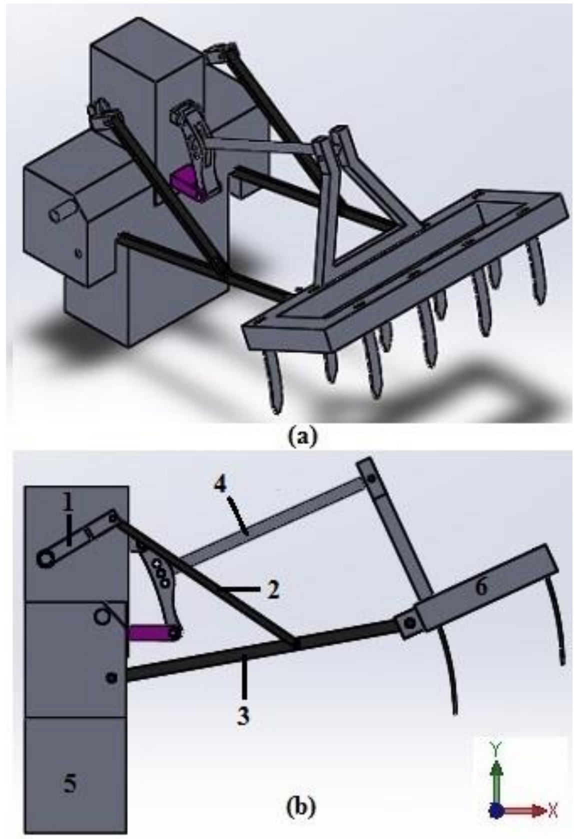

Fig. 3. Assembly of TPH system: (a) Isometric view, and (b) Left side view: 1= Lift arm, 2= Lift rod, 3= Lower arm, 4= Upper arm, 5= Tractor body, 6= Implement

In the TPH system, the rock shaft rotates in a fixed angular range; however, the movement range of the lower arm endpoints varies depending on the geometry of the connections. Therefore, in the laboratory test, it was determined that the rotation angle of the rock shaft varied from -6.29° to 57°. This range of angular rotation was implemented in the computer simulation using SolidWorks software. Subsequently, a motion study was conducted. In the motion study, a rotating motor was chosen for the rock shaft, with a rotating angle from -6.29° to 57°. At each value of lift arm inclination (θ), the coordinates of the hitch points and angles between arms (φ_1, φ_2, α, and β; Fig. 1) were measured to determine the locations of the vertical virtual hitch point, mechanical advantage, and the lifting capacity of the TPH system.

Vertical Virtual Hitch Point (VHP): The intersection point formed by the convergence of the lower arms and the upper arm (Dhruw *et al.*, 2018):

$$X_{VHP} = \frac{\tan\beta X_{P6} - Y_{P6} - \tan\alpha X_{P4} + Y_{P4}}{\tan\beta - \tan\alpha} \quad (1)$$

$$Y_{VHP} = \frac{\tan\beta Y_{P4} - \tan\alpha Y_{P6} + \tan\alpha \tan\beta (X_{P6} - X_{P4})}{\tan\beta - \tan\alpha} \quad (2)$$

Mechanical Advantage: It is defined as the ratio of output torque to input torque(Uicker, Pennock, & Shigley, 2016):

$$\mathrm{MA} = \frac{\text{output torque}}{\text{input torque}} = \frac{L_3 \sin\varphi 2}{L_1 \sin\,\varphi 1} \quad (3)$$

Lifting Force

There are two methods for measuring the static lifting capacity of the TPH system: one with a frame attached to the three-point hitch and one without a frame (OECD, 2012). The following equilibrium equations were applied to compute the lifting capacity of the TPH system in the configuration without the frame. The lifting capacity was calculated across the movement range under each test condition by fixing the torque transmitted by the hydraulic cylinder to the rock shaft. Consistent with OECD Code 2, the lifting capacity was defined as the minimum force value recorded within the movement range. The equations do not account for the inertial effects of the links. The equilibrium equations of lift arms are as follows (Avello Fernández *et al.*, 2022):

$$\begin{cases} F_{P1x} - F_{LR}\cos(\varphi_1 + \theta) = 0 \\ F_{P1y} - F_{LR}\sin(\varphi_1 + \theta) = 0 \\ M_{P1} - L_1 F_{LR}\sin(\varphi_1) = 0 \end{cases} \quad (4)$$

The equilibrium equations of the lower arms are as follows (Avello Fernández *et al.*, 2022):

$$\begin{cases} F_{P4x} - F_{LR}\cos(\varphi_2 \pm \alpha) = 0 \\ F_{P4y} + F_{LR}\sin(\varphi_2 \pm \alpha) = 0 \\ F_{LR}\sin(\varphi_2) l_3 - F_{lift}(l_4 \cos\alpha) = 0 \end{cases} \quad (5)$$

The variables F_{P1x} and F_{P1y} represent the horizontal and vertical parts of the force that the tractor applies to the lift arm, while F_{P4x} and F_{P4y} denote those same force components acting on the lower arm. Additionally, F_{LR} indicates the force applied by the lift rod to the lift arm, and M_{P1} refers to the torque delivered by the hydraulic system to the rock shaft. Based on these relationships, F_{lift} was determined by assigning a fixed value to the torque transmitted from the hydraulic system to the rock shaft (Fig. 4).

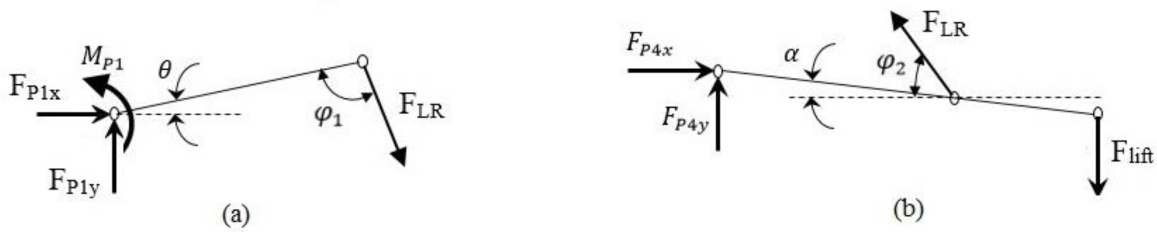

Fig. 4. Free Body Diagrams: (a) Lift and (b) Lower arms

During laboratory experiments, it was found that lifting a three-bottom plough weighing approximately 500 to 600 Kg requires the tractor's hydraulic system oil pressure to be 40 bar. At this pressure, the necessary torque on the rotating shaft was calculated to be 3.8 kN·m, and this value was included in all subsequent analyses.

Optimisation of the TPH system

To find the optimal design of TPH, we evaluated the effect of four independent variables of TPH design (including L_1, L_2, L_4, and L_3) on the lifting force. To do this, each independent variable was gradually changed from its existing value of TPH linkage while maintaining others constant. The lifting capacity of the TPH linkage was calculated for every simulation throughout the entire range of motion of the TPH linkage. Simulation outcomes were rigorously evaluated against ISO 730 standards (Table 1) via equations (6a)–(6h), enabling the exclusion of configurations failing to meet specified criteria. The design exhibiting the highest lifting capacity within these constraints was thereby identified as the optimal design.

Table 1- Dimensions of TPH parameters (ASABE Standards, 2007)

Variable	Value (mm)
l_b, l_u	550, 625
l_{14}	200
l_{15}	100
l_{18}	650
l_{19}	950
l_{20}	100

The constraint equations were (Molari *et al.*, 2014):

$$l_b \leq \left|P_{5,x}(c_1) - P_{PTO,x}\right| \leq l_u \quad (6a)$$

$$0 < P_{5,y}(c_4) \leq l_{14} \quad (6b)$$

$$\left|P_{5,y}(c_{6b}) - P_{5,y}(c_{6a})\right| \leq 2l_{15} \quad (6c)$$

$$P_{5.y}(c_3) - P_{5.y}(c_2) \geq l_{18} \quad (6d)$$

$$P_{5.y}(c_5) \leq l_{19} \quad (6e)$$

$$\sqrt{P_{5,x}^2(c_5) + P_{5,y}^2(c_5)} - r_{wr} \geq l_{20} \quad (6f)$$

$$L_{cv} \geq 0.9w \quad (6g)$$

$$\varphi_F(c_5) > 10^{\circ} \quad (6h)$$

The parameters c_1, c_2, c_3, c_4, c_5, c_{6a}, and c_{6b} are defined as follows: a medium length of lift rod with the lower arm positioned horizontally (c_1), at its lowest point (c_2), and at its highest point (c_3), with a maximum length of the lift rod and the TPH in the lowest position (c_4); a minimum length of the lift rod with the TPH at its highest position (c_5) and for the right lower arm (c_{6a}) and left lower arm (c_{6b}), the lower arm set horizontally, with the right lift rod fully extended and the left lift rod at its shortest length.

After finding the optimal design, the effect of independent variables of TPH design on the dependent variables (performance parameters), including the virtual hitch point, mechanical advantage, and lifting force, was analysed. For that purpose, each independent variable L_1, L_3, and L_4 was varied by ±10% from its optimal value while keeping the other variables constant to evaluate the dependent variables. In contrast, L_2 was varied by ±3.9% due to logistical constraints.

To identify the independent variable with the greatest impact on mechanical advantage and lifting force, the sensitivity index, defined as the percentage change in the dependent variable relative to the percentage change in the independent variable (±10 or 3.9% from the respective optimal value), was calculated using Eq. (7) (Molari *et al.*, 2014).

$$\text{Sensitivity Index} = \frac{\text{percentage change in the output variable}}{\text{percentage change in the input variable}} \quad (7)$$

Results and Discussion

Accuracy assessment

The SolidWorks simulation and laboratory tests were compared by plotting the height of the lower arm endpoint (H_{P5}) against the lift arm inclination. A good consistency was found between the laboratory and simulated measurements (Fig. 5). The laboratory tests determined that the height of the lower arm endpoint, movement range, and transport height of the existing TPH linkage were 23 mm, 58 mm, and 90 mm, respectively. Our findings indicated a discrepancy between the performance parameters of the existing three-point linkage and the ASABE standard requirements (ISO, 2009; ASABE Standards, 2007).

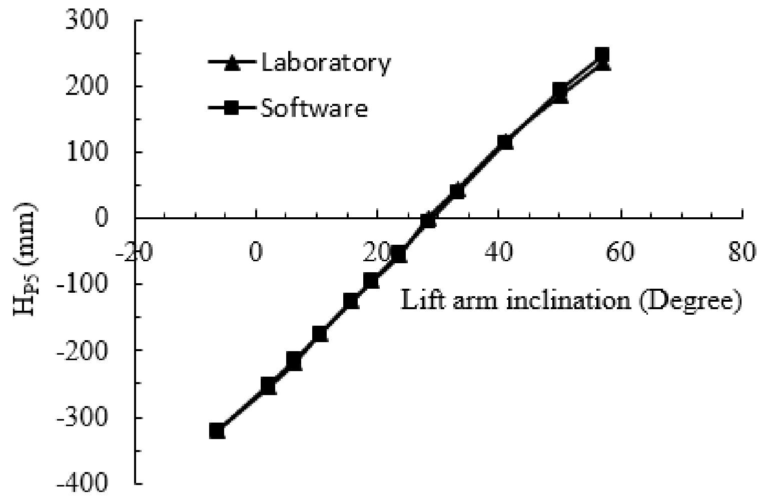

Fig. 5. Height of the lower arm endpoint (H_{P5}) versus lift arm inclination

Performance Analysis

Taking the rear axle centre as the origin, the motion paths of the TPH arms and the VHP positions were plotted for both the existing and optimised TPH systems, where the upper arm was attached to the midpoint of the pivot point (Fig. 6). The vertical convergence distances were found to be 2030 mm and 2041 mm in the existing and optimised designs, respectively, both of which are out of the specified range of the ASABE standard. According to the ASABE standard, it is recommended that the vertical convergence distance be between 0.9 and 3 times the tractor wheelbase for stable working conditions (ASABE Standards, 2007). It is worth mentioning that the VHP graphs were plotted from the horizontal position of the lower arms up to the end of the movement path of the TPH system.

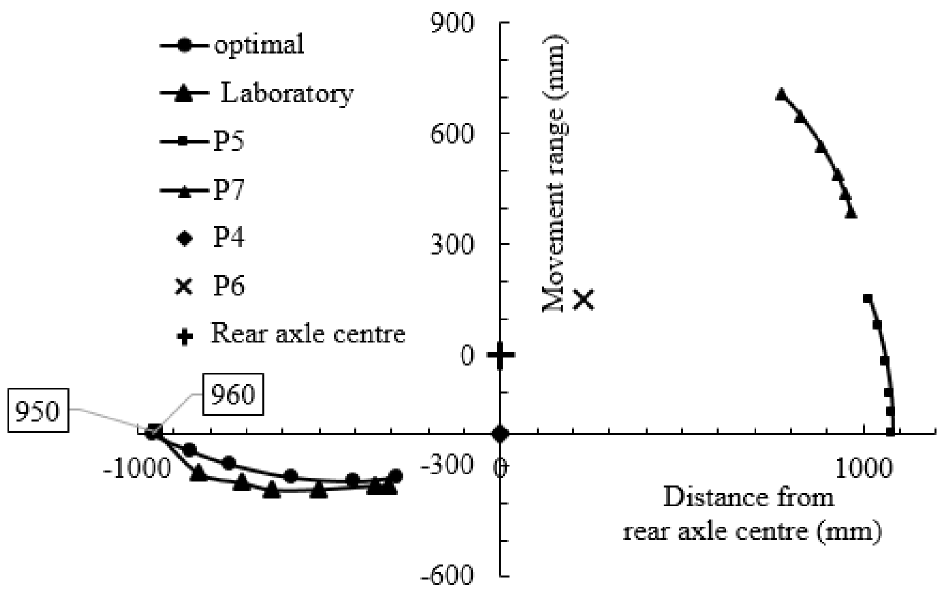

Fig. 6. Locations of VHP across the movement range

Figure 7 shows the effects of upper arm pivot points (P6) and mast heights (460 and

610 mm) on the vertical convergence distance and the position of the VHP. Results indicated that category-I implements should be utilised with the upper arm attached to the midpoint and lower point of the pivot point. In contrast, category-II implements should be used with the upper arm attached to the topmost point of the pivot point only. Prasanna Kumar (2015) stated that for Category-I implements, the upper arm can be connected to any of the pivot points. In contrast, for Category-II implements, the upper arm must be attached exclusively to the topmost pivot point.

The distance of the VHP increased more quickly when the upper arm was connected to the highest pivot point. Consequently, for heavy tillage implements in field operations, connecting the upper arm to the topmost pivot point is necessary to achieve improved weight transfer from the implement to the rear axle (Fig. 7).

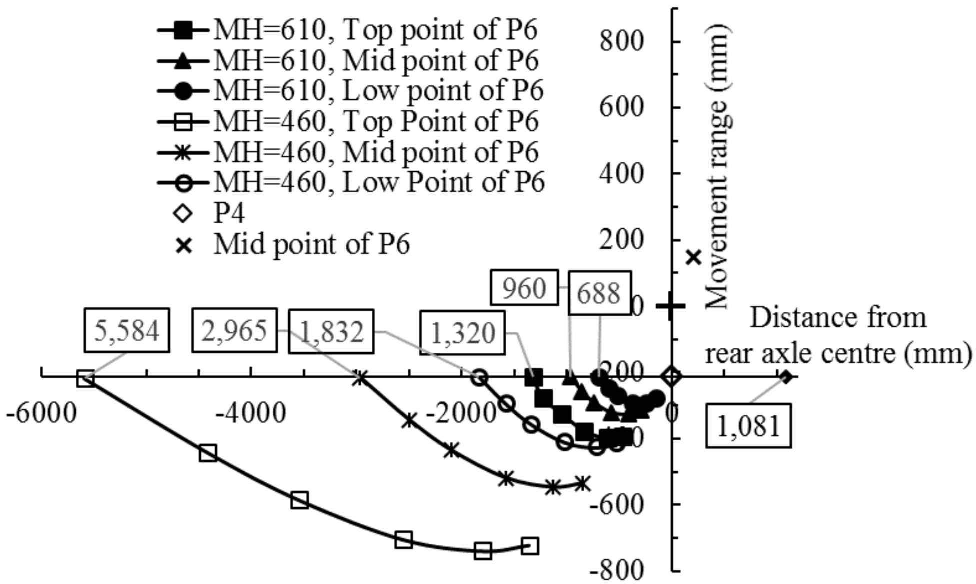

Fig. 7. Effects of the locations of P6 and mast height on the VHP

Additionally, the effects of independent variables (including L_1, L_2, L_3, and L_4) on the vertical convergence distance and the position of the VHP are indicated in Figs. 8-11. The results showed that L_4 has the greatest influence on the position of the VHP, with a 10% increase in L_4 leading to a 7.4% increase in the vertical convergence distance (Fig. 8). However, other parameters had no considerable effect.

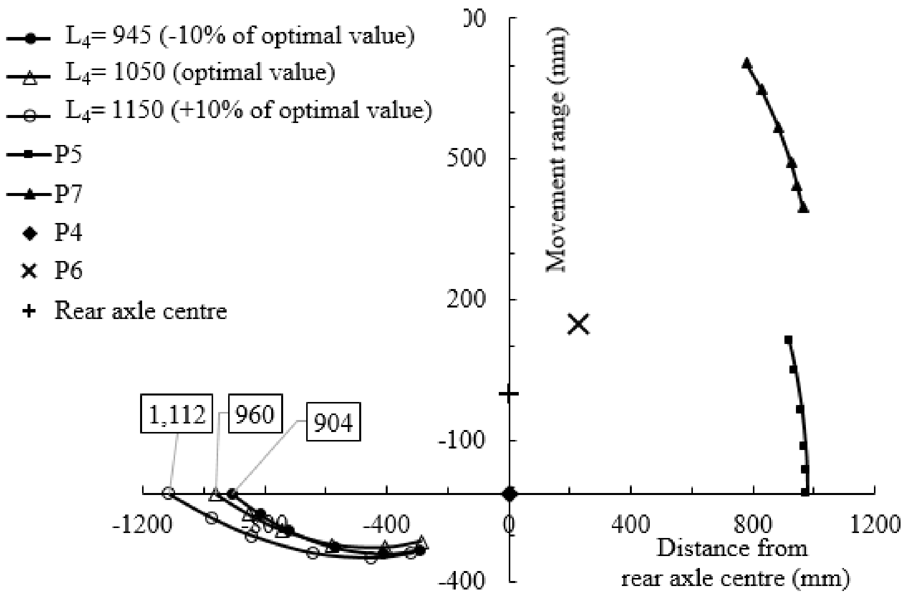

Fig. 8. Effect of different L_4 values on the VHP

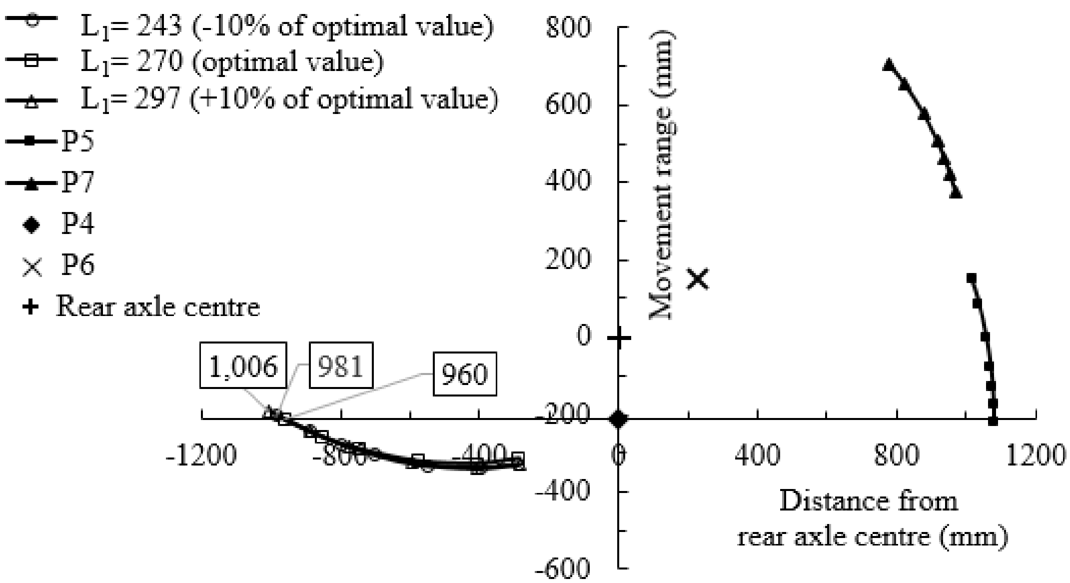

Fig. 9. Effect of different L_1 values on the VHP

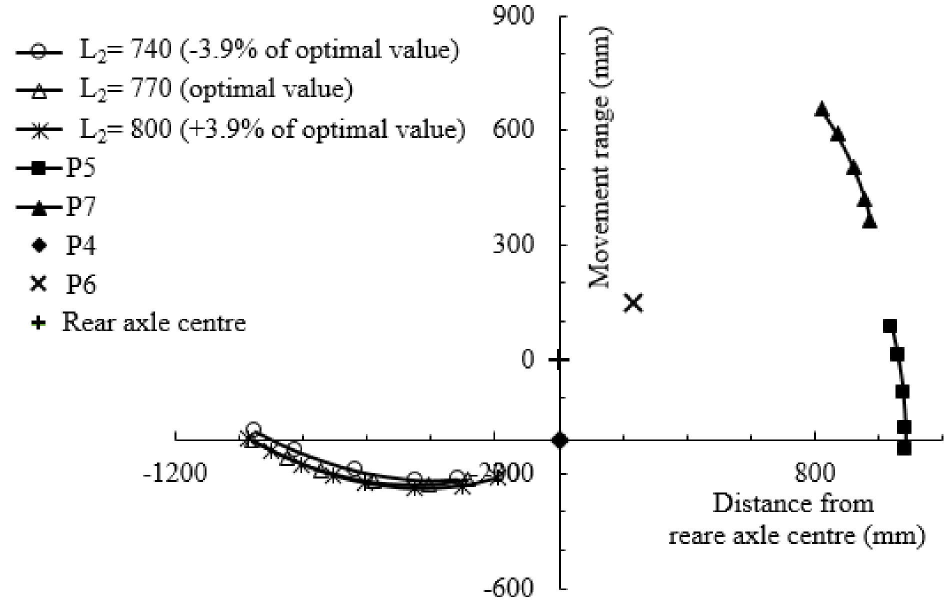

Fig. 10. Effect of different L_2 values on the VHP

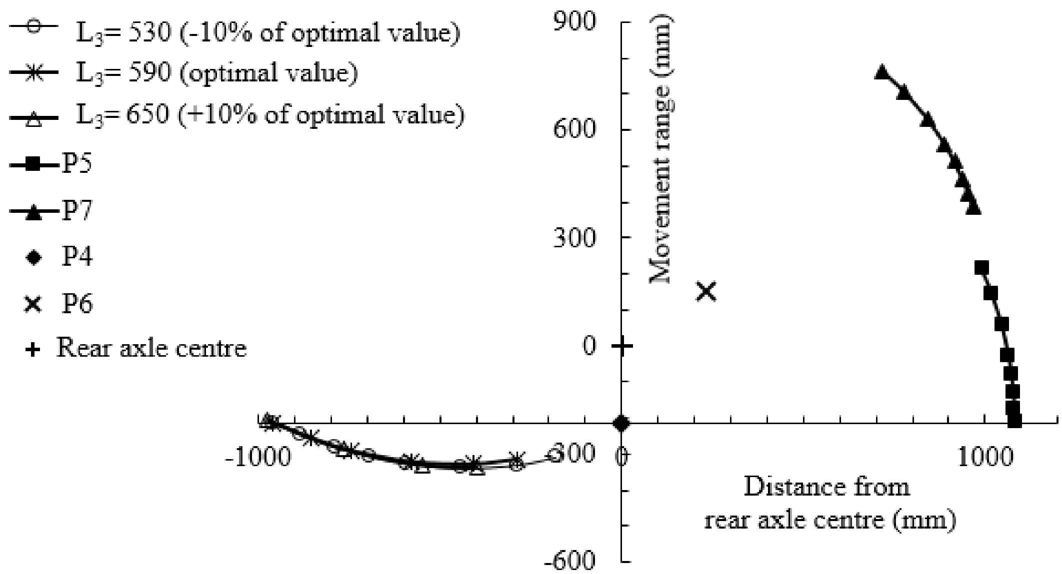

Fig. 11. Effect of different L_3 values on the VHP

It was observed that the mechanical advantage is highest when the lower arm endpoint is in its lowest position. As the height of the lower arm endpoint increases, the mechanical advantage decreases, reaching its minimum value approximately when the lower arms are in a horizontal position. Then, with a further increase in height, the mechanical advantage increases again. This pattern is consistent across all parameters (Figs. 12-15) and aligns with the findings reported by Dhruw *et al*. (2018) and Prasanna Kumar (2015).

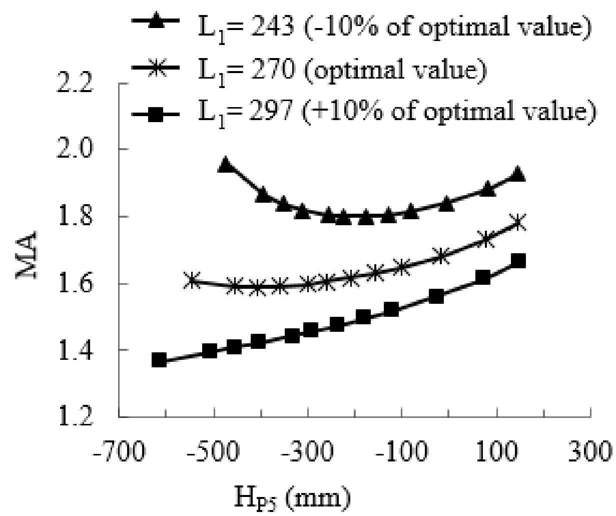

Fig. 12. Effect of different L_1 values on the mechanical advantage

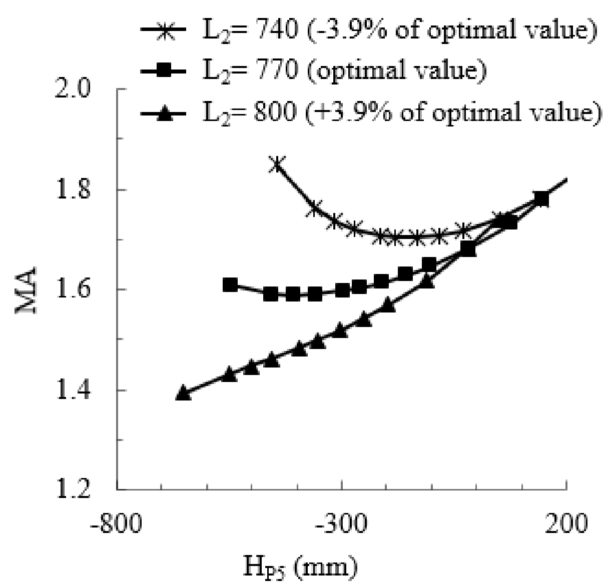

Fig. 13. Effect of different L_2 values on the mechanical advantage

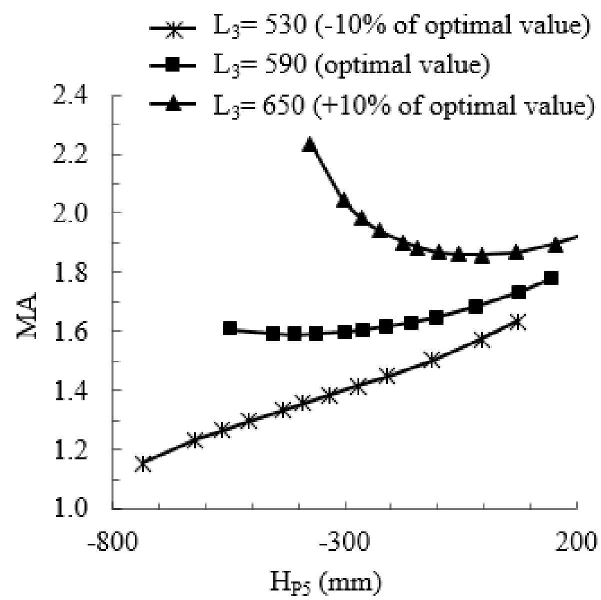

Fig. 14. Effect of different L_3 values on the mechanical advantage

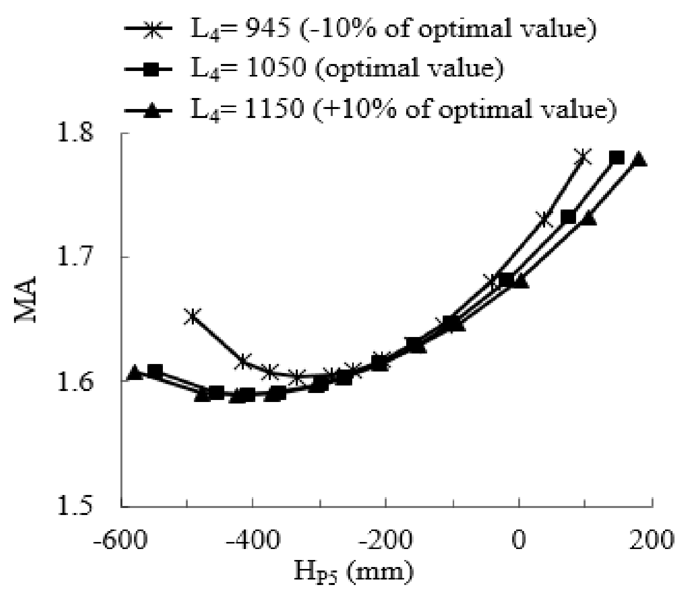

Fig. 15. Effect of different L_4 values on the mechanical advantage

The mechanical advantage for the optimised design was found to be 1.59, while for the existing design it was 1.71 (Table 2). However, the optimised design complies with all standard requirements, whereas specific parameters in the existing design exceed the standard limits.

The results of the sensitivity analysis showed that the lift rod length and the length of the lower arms are the most and least influential parameters on mechanical advantage, respectively (Table 2). By increasing the length of the lift rod arm and lower arms, the mechanical advantage reached -3.88 and zero, respectively (Table 2). This finding aligns with the results reported by Dhruw *et al.* (2014).

The lifting force versus the lifting height for both existing and optimal TPH was shown in Fig. 15. The lifting capacity, which equals the minimum force obtained in the movement range for the optimised TPH, was

5.8 kN. The corresponding H_{P5} was -297.9 mm. This force value was 8.4% lower than that of the existing three-point hitch (6.29 kN) (Fig. 16). However, the optimised design complies with all standard requirements, whereas specific parameters in the existing design exceed the standard limits.

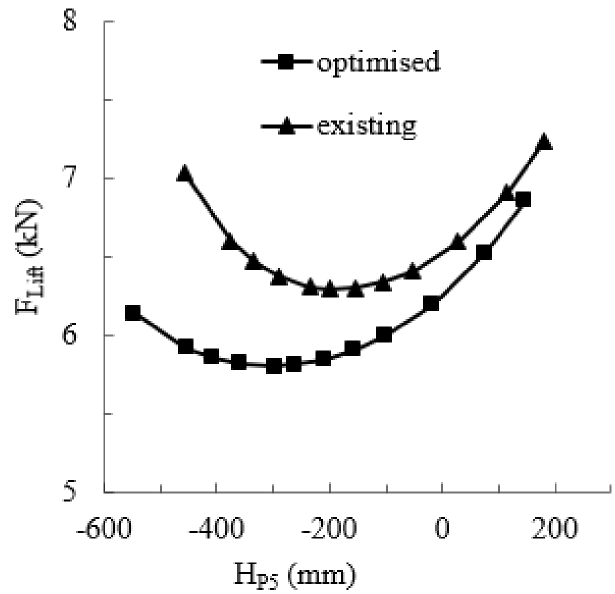

Fig. 16. Lifting force versus height of the lower arm endpoint (H_{P5}) for the optimised and existing TPH system

The effects of different TPH parameters on the lifting force across the movement range of lower arm endpoints were shown in Figs. 17 through 20. The lifting force goes down as the height of the lower arm endpoint increases. After reaching a certain height, when the lower arm is almost horizontal, the lifting force starts to rise again. This pattern is seen in all designs. These changes in lifting force are similar to the changes in mechanical advantage described earlier.

The lifting forces (F_{lift}) declined as L_1 and L_4 increased due to the rise in the resisting moment (Fig.17). As the length of L_3 increased, thereby extending the lifting force arm relative to the VHP, the resulting lifting forces were amplified (Fig. 18). This finding aligns with the results reported by Molari *et al.* (2014).

As shown in Fig. 17, an increase in L_4 relative to the optimal value of 1050 mm, this resulted in an 8.6% decline in the lifting force at the height of -306 mm. With the decline of L_4, the lifting force increased by up to 11.5% at a height of -281.5 mm. A decline of the L_3 corresponds to the optimal value of 590 mm, causing a 16.7% decrease in lifting force at the lifting height of -736.7 mm. With the increase of L_3, the lifting force increased up to 17.2% at the height of -97.8 mm (Fig.18). The increase in L_1 relative to the optimal value of 270 mm, it led to a 9.6% decrease in F_{lift} at the height of -401.4 mm. With the decrease of L_1, the lifting force increased up to 12.4% at the height of -177.9 mm (Fig.19). The increase in L_2 relative to the optimal value of 770 mm resulted in a 6.2% decrease in F_{lift} at the lifting height of -454.2 mm, however, a decrease in L_2 led to a 6.4% increase in the lifting force at the height of -179.9 mm (Fig. 20).

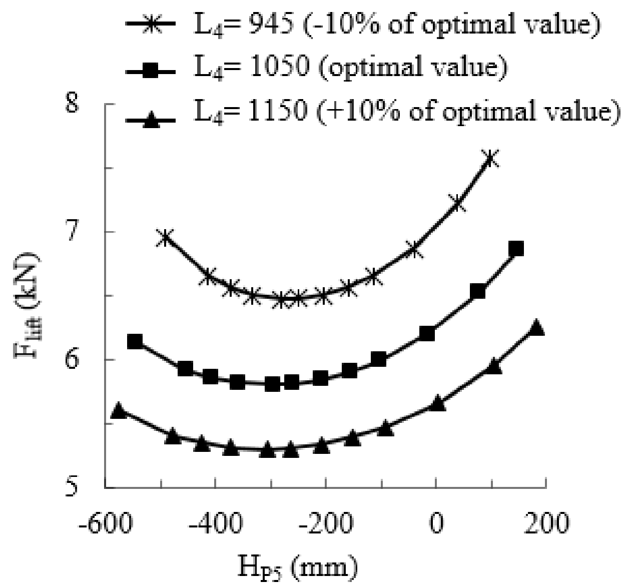

Fig. 17. Effect of different L_4 values on the F_{lift}

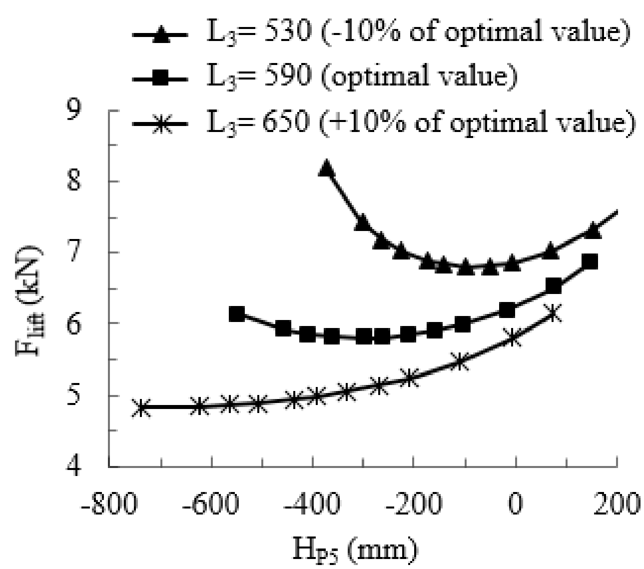

Fig. 18. Effect of different L_3 values on the F_{lift}

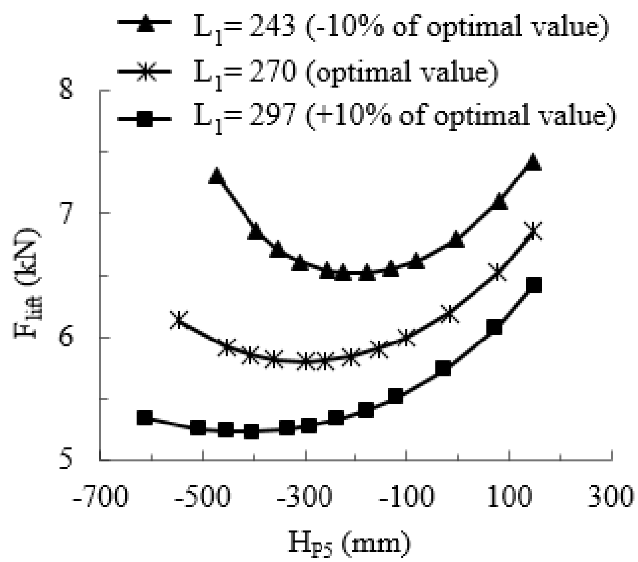

Fig. 19. Effect of different L_1 values on the F_{lift}

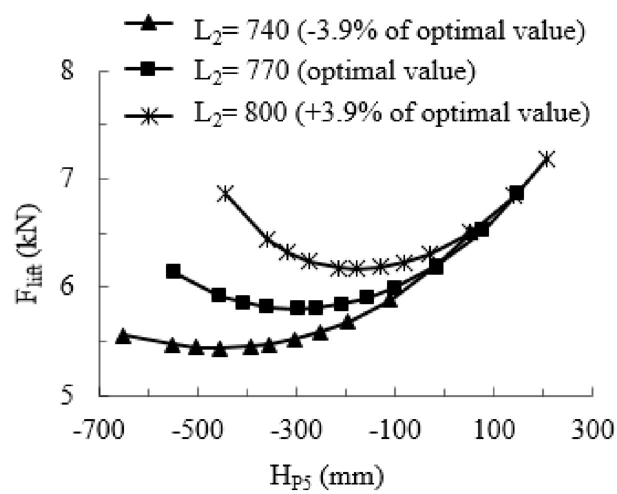

Fig. 20. Effect of different L_2 values on the F_{lift}

The sensitivity analysis results indicated that L_3 is the most influential parameter on the lifting force (Table 2). A 10% decrease in this parameter resulted in a sensitivity of -1.82, while a 10% increase yielded a sensitivity factor of 1.63. In contrast, the lower arm length had the least impact on lifting force (Table 2). This finding is consistent with the results of previous studies by Molari *et al.* (2014) and Avello Fernández *et al.* (2022).

It is important to note that altering the lift arm or lower arm lengths, or their connection points to the tractor body, is not a cost-effective option and has a limited effect on the lifting force. On the other hand, adjusting the connection point between the lift rods and the lower arms is inexpensive and easily achievable by adding extra holes or utilising slotted connections. Since this adjustment has the most significant impact on the lifting force, the best approach and recommendation for increasing the lifting force is to modify this parameter.

Table 2- Performance and sensitivity results of the three-point hitch system

Variable	Unit	Existing value	Optimal value	L_1		L_2		L_3		L_4	
				+10%	**-10%**	**+3.9%**	**-3.9%**	**+10%**	**-10%**	**+10%**	**-10%**
Minimum F_{lift}	kN	6.29	5.8	5.24	6.52	5.44	6.17	6.8	4.83	5.3	6.47
LHP height	mm		-297.9	-401.4	-177.9	-454.2	-179.9	-97.8	-736.7	-306	-281.5
Minimum MA	-	1.71	1.59	1.36	1.8	1.39	1.7	1.86	1.15	1.59	1.60
LHP height	mm		-297.9	-612.6	-177.9	-651.7	-131.7	-5.37	-736.7	-425.7	-281.5
VHP for MH = 610	-	2,030	2,041	2,050	2,061	1,980	2,055	2,056	2,040	2,192	1,984
Sensitivity of F_{lift}	-			-1.18	1	-1.78	1.49	1.63	-1.82	-1.09	0.94
Sensitivity of MA	-			-1.87	1.06	-3.88	1.61	1.61	-3.47	0	0.06

Conclusion

This study utilised SolidWorks software to model the motion of the TPH system, aiming to optimise the hitch geometry to meet ISO 730 standard requirements and improve the operational characteristics of the TPH. The main conclusions from the study are as follows:

- The SolidWorks simulation accurately predicted the TPH movement and geometries as validated by laboratory measurements, confirming the reliability of computer-aided design tools for analysing TPH systems.
- Geometric optimisation of the TPH parameters, particularly the lengths of the lift arm, the lift rod, the lower arms, and the connection point between the lift rod and the lower arm, resulted in a design that meets ASABE standard requirements. Despite an 8.4% reduction in lifting force, the optimised design ensures full compliance with standards and provides better operational stability.
- Modifying the position of the connection point between the lift rod and the lower arm is recommended as a cost-effective method to optimise TPH performance.
- The study supports the use of Category-I implements with the upper arm connected to the midpoint or lower point of the pivot points, whereas Category-II implements require connection at the topmost point of the pivot point to ensure effective weight transfer and operational stability during heavy tillage.
- Incorporating computer-aided design optimisation tools, such as SolidWorks, into the design process enables tractor manufacturing companies to achieve enhanced TPH geometries that comply with international standards.

Authors Contribution

The author solely contributed to all aspects of this manuscript, including conceptualisation, development of the methodology, data acquisition, data pre-processing and post-processing, software services, numerical and computer simulations, validation of results, and visualisation of the findings.

References

1. Ambike, S. S., & Schmiedeler, J. P. (2007). Application of Geometric Constraint Programming to the Kinematic Design of Three-Point Hitches. *Applied Engineering in Agriculture*, *23*(1), 13-21.
2. Anonymous. (2020). *Service Manual of MF285 Tractors. Iran Tractor Manufacturing company.www.itmco.ir (In Persian).*
3. ASABE Standards. (2007). *S217.12: Three-point free-link attachment for hitching implements to agricultural wheel tractors. St. Joseph, Mich.: ASABE.*
4. Avello Fernández, L., Maraldi, M., Mattetti, M., & Varani, M. (2022). A Computational Tool for Three-Point Hitch Geometry Optimisation Based on Weight-Transfer Minimisation. *Agriculture*, *12*(4), 460. https://doi.org/10.3390/agriculture12040460
5. Bauer, F., Porteš, P., Slimařík, D., Čupera, J., & Fajman, M. (2017). Observation of load transfer from fully mounted plough to tractor wheels by analysis of three point hitch forces during ploughing. *Soil and Tillage Research, 172,* 69-78. https://doi.org/10.1016/j.still.2017.05.007
6. Chukewad, Y. M., Chadha, S., Jagdale, K. S., Elkunchwar, N., Rosa, U. A., & Omohundro, Z. (2024). Tractor Three-Point Hitch Control for an Independent Lower Arms System. *AgriEngineering*, *6*(2), 1725-1746. https://doi.org/10.3390/agriengineering6020100
7. Dhruw, L. K., Pareek, C. M., & Singh, N. (2018). A Visual Basic Programme for Performance Evaluation of Three-point Linkage Hitch System of Agricultural Tractors. *Current Journal of Applied Science and Technology*, *28*(6), 1-12.

https://doi.org/10.9734/CJAST/2018/43491
8. ISO. (2009). *ISO 730: Agricultural wheeled tractors -Rearmounted three-point linkage-Categories 1N, 1, 2N, 2, 3N, 4N, and 4. Geneva, Switzerland: International Organization for Standardization.*
9. Jeon, H.-H., Jung, Y.-J., Siddique, M. A. A., Nam, K.-C., Kim, T.-B., Choi, C.-H., & Kim, Y.-J. (2019). Development and Validation of simulation model for three point-hitch during agricultural operation. *2019 Boston, Massachusetts July 7- July 10, 2019*. https://doi.org/10.13031/aim.201901032
10. Molari, G., Mattetti, M., & Guarnieri, A. (2014). Optimal Three-Point Hitch Design to Maximize Lifting Performance. *Transactions of the ASABE*, 371-379. https://doi.org/10.13031/trans.57.10353
11. OECD. (2012). *Code 2: OECD standard code for the official testing of agricultural and forestry tractor performance. Paris, France: Organization for Economic Cooperation and Development.*
12. Padhiary, M., Roy, P., & Kumar, K. (2025). Simulation Software in the Design and AI-Driven Automation of All-Terrain Farm Vehicles and Implements for Precision Agriculture. *Recent Progress in Science and Engineering*, *01*(02), 1-13. https://doi.org/10.21926/rpse.2502006
13. Pásztor, J., & Popa-Müller, I. (2021). Study of Three-Point Linkage of Power Machine. *Műszaki Tudományos Közlemények*, *14*(1), 60-64. https://doi.org/10.33894/mtk-2021.14.09
14. Pranav, P. K., Kumar, A., Ansh, A. K., & Kumar, S. (2024). Geometrical analysis of 3-point linkage of tractors for measurement and display of implement's working depth. *Research in Agricultural Engineering*, *70*(4), 237-244. https://doi.org/10.17221/23/2024-RAE
15. Prasanna Kumar, G. V. (2012). Development of a computer program for the path generation of tractor hitch points. *Biosystems Engineering*, *113*(3), 272-283. https://doi.org/10.1016/j.biosystemseng.2012.09.004
16. Prasanna Kumar, G. V. (2015). Geometric performance parameters of three-point hitch linkage system of a 2WD Indian tractor. *Research in Agricultural Engineering*, *61*(1), 47-53. https://doi.org/10.17221/79/2012-RAE
17. Selech, J., Ulbrich, D., Kęska, W., Staszak, Ż., Marcinkiewicz, J., Romek, D., & Rogoziński, P. (2019). Design of a cultivator mounted on a tractor with a power of up to 20 kW. *MATEC Web of Conferences*, *254*, 05003. https://doi.org/10.1051/matecconf/201925405003
18. Selvi, K. C., & Kabas, O. (2018). Use of Solidworks in designing agricultural machines (a sample: rotary tiller). *Journal of Engineering*, *Novemeber*, 101-107.
19. Singh, N., & Pandey, K. (2017). Development of Visual Basic Program to Design Front Mounted Three-Point Linkage for Higher Power Tractors. *Advances in Research*, *11*(2), 1-10. https://doi.org/10.9734/air/2017/35767
20. Uicker, J. J., Pennock, G. R., & Shigley, J. E. (2016). *Theory of machines and mechanisms* (fifth). OXFORD UNIVERSITY PRESS.
21. Wu, D., Zhang, Z., & Wang, Z. (2019). Application research of solidworks in modeling of straw carbonization preparation plant. *Journal of Physics: Conference Series*, *1303*(1), 012048. https://doi.org/10.1088/1742-6596/1303/1/012048

ارزیابی و بهینه‌سازی هندسه اتصال سه نقطه تراکتور MF475

نوروز مرادی نژاد[1*]

تاریخ دریافت: ۱۴۰۴/۰۵/۳۰
تاریخ پذیرش: ۱۴۰۴/۰۸/۱۸

چکیده

در سال‌های اخیر، استفاده از تراکتورهای کشاورزی باعث پیشرفت مکانیزاسیون مزارع شده است و سیستم اتصال سه‌نقطه‌ای (TPH) نقش مهمی در اتصال ادوات ایفا می‌کند. این مقاله بر روی بهینه‌سازی هندسه سیستم اتصال سه نقطه تراکتورمسی فرگوسن مدل ۴۷۵ (MF475) با استفاده از شبیه‌سازی در نرم‌افزار سالیدورک و اعتبارسنجی آن با اندازه‌گیری‌های کارگاهی متمرکز است. پارامترهای مستقل شامل: طول بازوی بالابر، طول بازوی رابط، طول بازوی پایینی و فاصله نقطه اتصال بازوی پایینی به بدنه تا نقطه اتصال بازوی رابط روی بازوی پایینی به‌منظور پیدا کردن طرح بهینه به‌صورت سیستماتیک تغییر داده شدند. علاوه‌براین، تأثیر پارامترهای مستقل بر روی پارامترهای عملکردی از قبیل: موقعیت نقاط اتصال مجازی، مزیت مکانیکی و نیروی بالابری تجزیه و تحلیل شدند. نتایج نشان داد که سیستم اتصال سه‌نقطه‌ای موجود در تراکتور MF475 با استانداردهای ASABE تفاوت‌هایی دارد، در حالی‌که طرح بهینه‌شده با این استانداردها مطابقت دارد. همچنین مشخص شد که طول بازوهای پایینی بیشترین تأثیر را بر روی موقعیت نقطه اتصال مجازی دارد. علاوه‌بر این، افزایش طول بازوی بالابر، طول بازوی رابط و طول بازوی پایینی باعث کاهش نیروی بالابری شدند. در مقابل، افزایش فاصله نقطه اتصال بازوی پایینی تا نقطه اتصال بازوی رابط روی بازوی پایینی باعث افزایش نیروی بالابری گردید. تحلیل حساسیت نشان داد که این فاصله، بیشترین تأثیر را بر روی نیروی بالابری و مزیت مکانیکی دارد.

واژه‌های کلیدی: سالیدورک، شبیه‌سازی، مزیت مکانیکی، نقطه اتصال مجازی، نیروی بالابری

۱- گروه مهندسی مکانیک بیوسیستم، واحد تبریز، دانشگاه آزاد اسلامی، تبریز، ایران
(*- نویسنده مسئول: Email: n.morad@iau.ac.ir)

https://doi.org/10.22067/jam.2025.95018.1422